BRBs uncertainty propagation in seismic retrofit of RC structures

Needhi Kotoky
Post Doctorate Fellow, Department of Civil Engineering, Indian Institute of Technology Bombay, Mumbai, India

Fabio Freddi
Lecturer in Structural Design, Department of Civil, Environmental & Geomatic Engineering, University College of London, London, UK

Jayadipta Ghosh
Assistant Professor, Department of Civil Engineering, Indian Institute of Technology Bombay, Mumbai, India

Meera Raghunandan
Assistant Professor, Department of Civil Engineering, Indian Institute of Technology Bombay, Mumbai, India

ABSTRACT: Passive control systems, such as buckling restrained braces (BRBs), have emerged as an efficient tool for the seismic response control of new and existing structures by providing strength and stiffness to buildings, in addition to high and stable energy dissipation capacity. Systems equipped with BRBs have been widely investigated in literature, however, only deterministic description of the BRBs' properties is usually considered. These properties are provided by the manufacturer and are successively validated by qualification control tests. The acceptance criteria specified by codal standards allows for some variation in the response of a single BRB by introducing a tolerance limit. Therefore, the 'real' properties of these devices could differ from the design values. This difference can affect the seismic response and potentially lead to an undesired seismic performance at the global level. This paper provides some preliminary insights on the influence of the BRBs' uncertainty on the seismic response of a retrofitted RC frame. For the case-study, a benchmark two-dimensional RC frame is considered. A single retrofit condition is analyzed and the BRBs' uncertainty is defined according to the tolerance limits of devices' quality control tests. Cloud analysis and probabilistic seismic demand models are used to develop fragility functions for four different damage states. Fragility curves are defined for the bare and retrofitted frame while considering both the design and the 'real' values of the BRBs properties. The preliminary results show that the BRBs' uncertainty could lead to an increase of the vulnerability up to 26.80% for the considered case-study.

1. INTRODUCTION

Many reinforced concrete (RC) frame buildings designed prior to the introduction of modern seismic codes are significantly vulnerable to earthquake loads due to their reduced ductility capacity. The seismic performance of these frames can be improved by seismic retrofitting techniques. Amongst many, the use of dissipative braces has demonstrated to be effective in reducing the seismic response and hence in protecting structural and non-structural building components (Zona and Dall'Asta 2012). These braces provide a supplemental path for the earthquake induced lateral loads, thereby enhancing the seismic behavior of the frame by adding energy dissipation capacity and, in some cases, stiffness to the bare frame

The use of supplemental energy dissipation systems has been widely investigated in literature (Di Sarno and Manfredi 2010, Freddi et al. 2013, Tubaldi et al. 2016, Baiguera et al. 2016), although, only a deterministic description of the dampers' properties is considered. Design properties for the dampers are provided by the manufacturer and, successively assessed by qualification control tests where tolerance limits are considered. The effectiveness of damping devices and design method, in mitigating the seismic response may be affected by the variation in damper properties that are introduced due to tolerance limits as investigated by Dall'Asta et al. (2017) and Scozzese et al. (2019) while considering viscous dampers.

Buckling restrained braces (BRBs) are a type of supplemental damping devices where a sleeve provides buckling resistance to an unbonded core that resists the axial stress. As buckling is prevented, BRBs behave in a similar way in tension and in compression allowing the development of stable hysteretic cycles, providing significant energy dissipation capacity (Zona and Dall'Asta 2012). This paper provides some preliminary insights on uncertainty stemming from BRB parameters on the seismic response and fragility of a RC frame building. A benchmark two-dimensional RC frame is used as case-study and a single retrofit condition is analyzed here. In this case, the BRBs are designed such that the base shear capacity proportion between the BRBs system and the existing frame is equal to 1.

The paper is organized as follows: at the onset, the paper introduces the geometry and the numerical modeling of a case-study non-ductile RC moment resisting frame (MRF) along with validation using experimental results. The subsequent sub-section describes retrofitting of the case-study frame with dissipative braces consisting of BRBs and elastic brace. The next section presents the comparison of seismic vulnerability of bare frame and retrofitted frame. This section also presents the impact of uncertainty in BRBs parameters on seismic fragility of retrofitted frame. The paper ends with conclusions and discussion for the future work.

2. CASE-STUDY BUILDING

2.1. Case-study building frame

Figure 1 shows the three-bay three-story non-ductile RC MRF used as case-study building. The choice of this case-study as benchmark is related to the availability of detailed experimental data (Aycardi et al. 1994, Bracci et al. 1995), allowing a reasonably approximate validation of the numerical models at global and local level. This building frame has also been widely used in previous (Freddi et al. 2017, Jeon et al. 2015). The height of each story within the frame is 3.66 m, while the bay width is of 5.49 m. Columns have square sections of 300 × 300 mm^2 while beams dimensions are 230 × 460 mm^2. The building frame has only been designed for gravity loads without considering seismic detailing, by using design guidelines prior to the introduction of modern seismic codes. The concrete compressive cube strength is 24 MPa and the reinforcing bars are Grade 40 steel with a yield strength of 276 MPa. Additional information on the case-study frame can be found in Bracci et al. (1995). D-1 to D-3 reported in Figure 1 indicate the placement of BRBs along the height of the retrofitted frame.

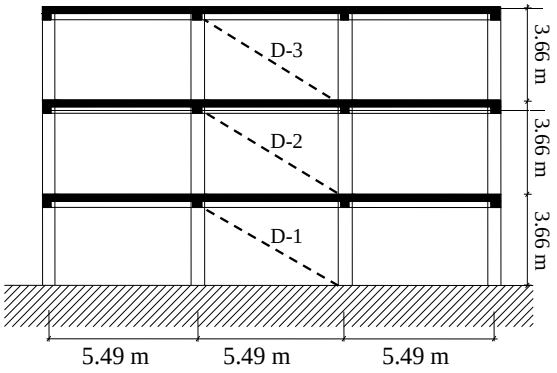

Figure 1 Case-study frame layout (adapted from Bracci et al. 1995).

2.2. Numerical model

A two-dimensional finite element (FE) model of the structure is developed in OpenSees (McKenna et al. 2006). The *beamWithHinges* (Scott and

Fenves 2006) element, used to model the frame's beams and columns comprises of a linear elastic region in the central part and two fiber section at element ends to simulate the behavior of the plastic hinge zones. The plastic hinge length is defined according to Panagiotakos and Fardis (2001). The effective flexural stiffness of the elastic part is calculated using moment-curvature analysis of the section, considering the axial force level induced by dead loads. Column and beams cross-sections at element end are defined using *FiberSection* with rectangular concrete patches and layers of reinforcement. Confined and unconfined concrete for the fiber sections, are modeled using the nonlinear degrading *Concrete02* material model. Longitudinal reinforcements are modeled using the *uniaxialMaterial Hysteretic* whose parameters controlling pinching, damage and degraded unloading stiffness are calibrated using experimental results. In the beams, the contribution of the slab is modeled considering T-sections with effective width considered as 4 times the width of the beam.

The shear response in the columns is simulated using a zerolength shear spring positioned at the column top. The *uniaxialMaterial LimitState* developed by Elwood (2004) is implemented for shear spring model. The joint model includes a multi-linear response envelope and a tri-linear unload-reload path. This model is implemented using the *Pinching4* material (Lowes et al. 2004). The joint region is modeled using a two-node, zero-length rotational joint spring and four rigid offsets (Alath et al. 1995, Jeon et al. 2015). The joint response is simulated using a material model that defines joint moment versus rotation. As demonstrated in Celik and Ellingwood (2008), the joint moment-rotation relationship is determined from the joint shear stress-strain relationship using equilibrium and compatibility.

Bracci et al. (1995) reports the results of the experimental tests carried on the 1:3 scale of benchmark frame. The results of snap back and white noise tests provide information on the frame vibration periods and the modal shapes. The first three natural periods measured in the experimental test results (0.537, 0.176 and 0.119 s) are in close agreement with the periods provided by the 1:3 scale FE model with uncracked gross stiffness properties (0.552, 0.172, and 0.100 s). A satisfactory agreement is also observed corresponding to the first three modal shapes.

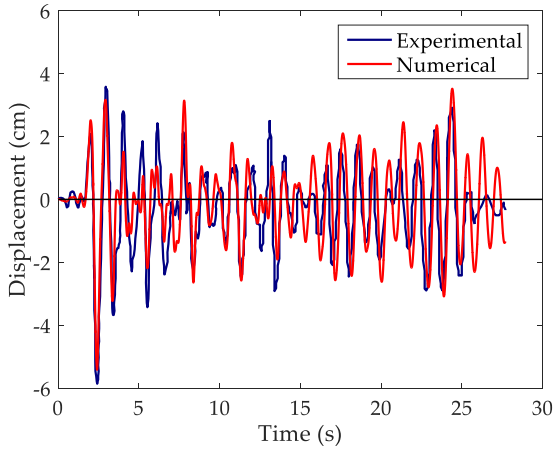

Figure 2 Comparison of numerical and experimental shaking table tests results: top story displacement for PGA = 0.30g

Shaking table tests results reported in Bracci et al. (1995) describes the time-history of the 1:3 scaled benchmark frame response under the Kern County 1952, Taft Lincoln School Station, N021E component record scaled for different levels of the seismic intensity with peak ground acceleration (PGA) of 0.05g, 0.20g and 0.30g. Figure 2 compares the top story displacements of the 1:3 scaled experimental and numerical model for the intensity level with PGA = 0.30g. In the FE model, damping sources other than the hysteretic dissipation of energy are modeled through the Rayleigh damping matrix. The values of the mass-related and stiffness-related damping coefficients are obtained from the snap back test given in Bracci et al. (1995). These values are 2.5% and 4.8% respectively for the first two modes and allow to calculate the Rayleigh damping coefficients for time history analysis. The numerical results indicate a satisfactory

agreement with the experimental results across all three intensity levels.

Although not shown here for brevity, the numerical and experimental behavior of isolated columns and beam to column joints under cyclic loading is in satisfactory agreement. Such comparisons, provide confidence to the local response prediction capabilities simulated by the numerical model.

2.3. Frame retrofitted with BRBs

As shown in Figure 1, the case-study frame is retrofitted using BRBs placed in the central bay at each story. The dissipative braces are composed by an elasto-plastic dissipative device (BRB) arranged in series with an elastic brace exhibiting adequate over-strength (Zona and Dall ' Asta 2012). This arrangement allows the independent calibration of the stiffness (K_c^i) and strength (F_c^i) of the dissipative diagonal braces. The distribution of the stiffness K_c^i at each story is designed in order to keep the first modal shape of the bare frame unchanged after the retrofit implementation (Dall'Asta et al. 2009, Ragni et al. 2011). This avoids drastic changes to the internal action distribution in the frame, at least in the range of the elastic behavior. Moreover, the distribution of the strength F_c^i is designed with the aim of obtaining the simultaneous yielding of the devices at all the stories so that the global ductility of the bracing system is the same as the ductility of the single braces. More details about the design method employed can be found in Dall'Asta et al. 2009.

The bracing system can be designed for different values of the strength proportion coefficient (α) that defines the ratio between the seismic base shears carried by the BRB frame and MRF respectively. This study considers the value of α as 1. Another important parameter that control the design is the ductility of the dissipative brace (μ_{BRB}) that has been assumed equal to 15 in this study (Uang and Nakashima 2004). Table 1 shows the properties of dissipative braces K_c^i and F_c^i at each story together with the material's yield strength ($f_{y,BRB}$), the area (A_{BRB}) and length (L_{BRB}) of the BRB device. The device behavior is modeled using *SteelBRB* material model in OpenSees (Gu et al. 2014).

Table 1 BRBs design properties

Floor No.	F_c^i [kN]	K_c^i [kN/m]	$f_{y,BRB}$ [MPa]	A_{BRB} [mm^2]	L_{BRB} [mm]
1	207.9	45967.4	250.0	831.6	2799.3
2	178.9	30940.0	250.0	715.7	3579.2
3	103.0	28242.4	250.0	412.0	2257.4

3. SEISMIC FRAGILITY ASSESSMENT

Seismic fragility curves indicate conditional probabilistic statements that depict the likelihood of meeting or exceeding a particular damage state given the ground motion intensity measure (*IM*), chosen as spectral acceleration corresponding to the first structural period in this study. The maximum interstory drift ratio (ISD) is chosen as the engineering demand parameter. Samples of the demand for the ISD are obtained using cloud analysis and analytically described by probabilistic seismic demand models (PSDMs) (Cornell et al. 2002). The seismic capacity is defined by threshold values correlated to damage states as discussed in the subsequent section. Following the lognormality of the demand and capacity estimates, seismic fragility for a given damage state *ds* is computed as:

$$P\left[DS \geq ds \middle| IM \right] = \Phi\left(\frac{\ln(IM) - \ln(med_{ds})}{\zeta_{ds}} \right) \quad (1)$$

where, Φ is the cumulative distribution function of a standard normal distribution, med_{ds} is the median of fragility and ζ_{ds} is the dispersion of fragility for a particular damage state *ds*.

3.1. Ground motion selection

A set of 150 unscaled ground motion records from the SIMBAD database (Smerzini et al. 2014) provides a statistically significant number of strong-motion records of engineering relevance. This database includes shallow crustal earthquakes with moment magnitudes ranging from 5 to 7.3 and epicentral distances smaller than 35 km.

3.2. Limit state capacity models

ISDs are used to provide a quantitative descriptions of the discrete damage states in the building as: Slight, Moderate, Extensive and Complete (FEMA 2003). Damage state thresholds are defined based on a pushover analysis and by monitoring the qualitative behavior of the structural elements (Dolšek and Fajfar 2008, Rossetto et al. 2016). The qualitative description of the elements' behavior associated with each damage states is reported in Table 2 alongwith median values of the maximum ISDs.

Table 2 Damage states description and ISD limits

Damage States	Description	Maximum ISD (%)
Slight	Start of yielding of column	0.77
Moderate	Yielding of all columns at one floor	1.02
Extensive	Crushing of concrete in 50 % of columns at one floor	1.98
Complete	Initiation of shear failure	4.34

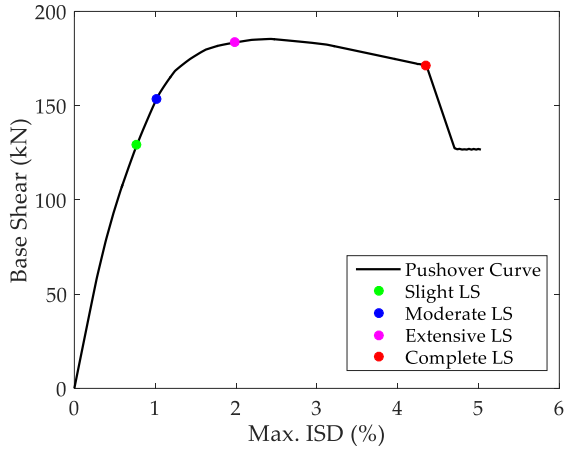

Figure 3 Pushover curve and limit state (LS) mapping

Figure 3 reports the pushover curve of the case-study bare frame together with the maximum ISDs for each of the four limit states. Since the BRBs design method ensure that there is no variation of the mode shape, the max ISDs used for the definition of the LSs doesn't change with retrofit of the frame. A dispersion β_C of 0.3 is assumed in the definition of the capacity values in order to account for the uncertainty associated the definition of the damage states.

3.3. Seismic fragility

Error! Reference source not found.(a) shows the PSDMs for the bare and retrofitted frame with BRB parameters held at design values. The markers in the figure represent the *IM-EDP* pairs obtained from 150 non-linear time history analysis (NLTHA) and the corresponding PSDMs. T_1 is equal to 1.20s and 0.60s respectively for the bare and retrofitted frame.

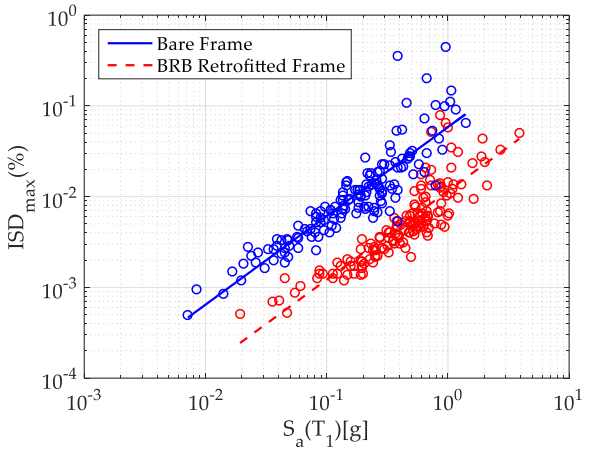

(a)

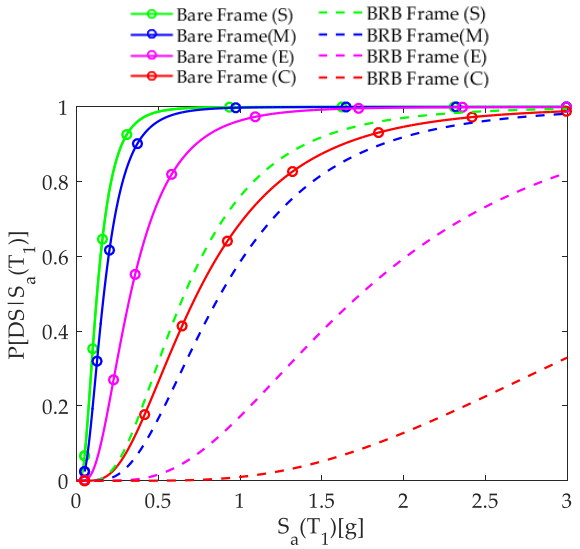

(b)

Figure 4 (a) PSDMs and (b) Seismic fragility curves for bare and retrofitted frame for Slight(S),

Moderate(M), Extensive(E) and Complete(C) damage states

Error! Reference source not found.(b) shows fragility curves for the bare and retrofitted frame for the four damage states. A significant increase in median spectral acceleration (*i.e.*, the $S_a(T_1)$ corresponding to 50% probability of exceeding a particular damage state) is observed for retrofitted frame as compared to bare frame. This percentage increase comes out to be 407.7%, 417.6%, 427.3% and 424.3% for Slight, Moderate, Extensive and Complete damage states. Figure 4 doesn't provide the information regarding the effectiveness of the retrofit since the time-period of the bare and retrofitted frame are different and structural dependent *IM* ($S_a(T_1)$) is employed to monitor seismic demand. Such comparison is beyond the objectives of the present work and more detail on this can be found in Freddi et al. (2013).

3.4. Influence of BRBs uncertainty on seismic fragility

As mentioned, BRBs properties are provided by the manufacturer and successively assessed by qualification control tests where the acceptance criteria allow some variation in the response of the single device by introducing a tolerance limit. The effect of such variation with respect to the design values is assessed by considering the uncertainty of the main parameters influencing the BRBs response, such as the device area (A_{BRB}) and the device material yield strength ($f_{y,BRB}$). No correlation is assumed between the uncertainty affecting the devices at different stories. The lower and upper limit of the design parameters (A_{BRB}, $f_{y,BRB}$) are chosen such that the maximum force recorded in the braces does not deviate from the design value more than ±15% (ASCE/SEI 41-13) according to the tolerances defined in the acceptance criteria.

In the preliminary analysis, the condition with design parameters is compared with 8 selected combination as given in Table 3. The design area of device (A_{BRB}) is increased or decreased by 15% at all the three stories. This variation affects both the F_c^i and the K_c^i. The variation of the $f_{y,BRB}$ is neglected in this study assuming that the manufacturer uses the same material for the devices at all stories.

Table 3 Combination of BRB uncertainty

Combination	A_{BRB1} (%)	A_{BRB2} (%)	A_{BRB3} (%)
1	15	15	15
2	-15	-15	15
3	15	-15	-15
4	15	-15	15
5	-15	15	15
6	15	15	-15
7	-15	-15	-15
8	-15	15	15

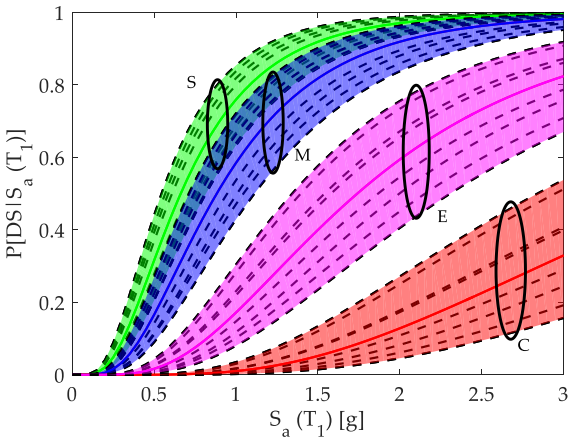

Figure 5 Seismic fragility of retrofitted frame for the 8 combinations of BRB parameters for Slight (S), Moderate (M), Extensive (E) and Complete (C) damage states

Fragility curves are derived considering the spectral acceleration at the first modal period of the frame with BRBs (properties set at design values) as the intensity measure. It is worthwhile to note that the structural time periods of the eight case-study buildings with different BRB combinations (as indicated in Table 3) vary negligibly. Figure 5 shows the comparison of the fragility curve bands for all the considered combinations. Fragility curves are reported for all the damage states and a significant variation of the retrofit performance due to the BRBs uncertainty

is observed. The bold line in between all the four bands corresponds to the case with the design values and the colored band with dotted lines corresponds to the 8 combinations of Table 3. Table 4 reports the median values of $S_a(T_1)$ corresponding to the 50% probability of failure together with the dispersion values of the lognormal function for both the design and worst-case scenario (combination 8 in Table 4). It is observed that consideration of uncertainty within BRB properties at different stories results in decrease in the median $S_a(T_1)$ across all damage states. The observed percentage decrease in the median value of fragility for the worst combination property as compared to the design case are of 16.67%, 19.31%, 22.98% and 26.80% for four damage states. A slight increase in dispersions values is also observed.

Table 4 Seismic fragility parameters for design and 'real' (worst combination) retrofitted case

Damage states	Design properties		'Real' properties for the worst combination	
	med_{ds}	ζ_{ds}	med_{ds}	ζ_{ds}
Slight	0.66	0.57	0.55	0.60
Moderate	0.88	0.57	0.71	0.60
Extensive	1.74	0.57	1.34	0.60
Complete	3.88	0.57	2.84	0.60

4. CONCLUSIONS

BRBs have emerged as efficient tools for improving the seismic performance of non-ductile existing buildings. Once designed and produced by the manufacturer, these devices should conform with the acceptance criteria specified by code standards and their properties should not differ from the design more than a tolerance limits. The objective of this paper is to investigate the influence of the device parameters uncertainty and code tolerance limits on the seismic response of non-ductile RC frame buildings retrofitted with BRBs. Seismic fragility curves are derived for a case-study bare and retrofitted frame where BRBs are installed. The results show the effect of the BRBs uncertainty on the seismic response of the system. In this preliminary analysis, the design condition is compared with 8 possible worst-case scenarios due to the devices' uncertainty. Variability of the BRBs parameters within the code tolerance limits shows a significant variation of the seismic performance of the retrofitted frame. The shift in the vulnerability highlights the importance of considering BRBs parameter uncertainty within the framework of seismic vulnerability assessment of retrofitted frames.

5. ACKNOWLEDGEMENT

The financial support provided by UGC-UKIERI joint research programme (Grant No. 2017-UGC-10070) is gratefully acknowledged.

6. REFERENCES

Alath, S., and Kunnath, S.K. (1995). "Modeling inelastic shear deformations in RC beam–column joints. In: Engineering Mechanics", In *Proceedings of 10th Conference of Engineering Mechanics*, University of Colorado, Boulder, CO, 822–5.

ASCE 41-13. (2013). "Seismic Evaluation and Retrofit Rehabilitation of Existing Buildings", *American Society of Civil Engineers*, Reston, VA.

Aycardi, L.E., Mander, J.B., and Reinhorn, A.M. (1994). "Seismic resistance of reinforced concrete frame structures designed only for gravity loads: experimental performance of subassemblages." *ACI Structural Journal*, 91(5), 552–563.

Baiguera, M., Vasdravellis, G., and Karavasilis, T.L. (2016). "Dual seismic-resistant steel frame with high post-yield stiffness energy-dissipative braces for residual drift reduction." *Journal of Constr. Steel Research*, 122, 198–212.

Bracci, J.M., Reinhorn, A.M., and Mander, J.B. (1995). "Seismic resistance of reinforced concrete frame structures designed for gravity loads: performance of structural system." *ACI Structural Journal*, 92(5), 597–608.

Celik, O.C., and Ellingwood, B.R. (2008). "Modeling beam–column joints in fragility assessment of gravity load designed reinforced concrete frames" *Journal of Earthquake Eng.*, 12(3), 357–81.

Cornell, C., Jalayer, F., Hamburger, R. O., and Foutch, D. A. (2002). "Probabilistic basis for 2000 SAC federal emergency management agency steel

moment frame guidelines." *Journal of Structural Eng.*, 128(4), 526–533.

Dall'Asta, A., Scozzese, F., Ragni, L., and Tubaldi, E. (2017). "Effect of the damper property variability on the seismic reliability of linear systems equipped with viscous dampers" *Bulletin of Earthquake Eng.*, 15(11): 5025-5053

Dall'Asta, A., Ragni, L., Tubaldi, E., and Freddi, F. (2009). "Design methods for existing RC frames equipped with elasto-plastic or viscoelastic dissipative braces" *In Proceedings of XIII Convegno Nazionale ANIDIS*, Bologna, Italy.

Di Sarno, L., and Manfredi, G. (2010). "Seismic retrofitting with buckling restrained braces: Application to an existing non-ductile RC framed building", *Soil Dynamics & Earthquake. Eng.*, 30(11), 1279–1297.

Dolšek, M., Fajfar, P. (2008). "The effect of masonry infills on the seismic response of a four-storey reinforced concrete frame – a deterministic assessment" *Eng. Structure*, 30(7), 1991–2001.

Elwood, K.J. (2004). "Modeling failures in existing reinforced concrete columns" *Canadian Journal of Civil Eng.*, 31(5), 846–59

FEMA (2003). HAZUS-MH MR4 Technical manual-Earthquake model. *Federal Emergency Management Agency*, Washington, DC.

Freddi, F., Tubaldi, E., Ragni, L. and Dall'Asta, A. (2013). "Probabilistic performance assessment of low-ductility reinforced concrete frames retrofitted with dissipative braces" *Earthquake Eng. and Structural. Dynamics*, 42, 993–1011.

Freddi, F., Padgett, J.E. and Dall'Asta, A. (2017). "Probabilistic seismic demand modeling of local level response parameters of an RC frame" *Bulletin of Earthquake Eng.* 2017, 15:1–23.

Gu, Q., Zona, A., Peng, Y., and Dall'Asta, A. (2014). "Effect of buckling-restrained brace model parameters on seismic structural response" *Journal of Construction Steel Research*, 98,100-113.

Jeon, J-S., Lowes, L. N., DesRoches, R., and Brilakis, I. (2015). "Fragility curves for non-ductile reinforced concrete frames that exhibit different component response mechanisms" *Eng. Structures*, 85: 127–143

Lowes, L.N., Mitra, N., and Altoontash, A. (2004). "A Beam-Column Joint Model for Simulating the Earthquake Response of Reinforced Concrete Frames" PEER Report 2003/10.

McKenna, F., Fenves, G.L., and Scott, M.H. (2006). "Open system for earthquake engineering simulation", University of California, Berkeley, CA.

Panagiotakos, T.B., and Fardis, M.N. (2001). "Deformation of reinforced concrete members at yielding and ultimate" *ACI Structural Journal*, 98(2), 135–148.

Ragni, L., Zona, A., Dall'Asta, A. (2011). "Analytical expressions for preliminary design of dissipative bracing systems in steel frames", *Journal of Construction Steel Research*, 67(1), 102-113.

Rossetto, T., Gehl, P., Minas, S., Galasso, C., Duffour, P., Douglas, J., Cook, O. (2016). "FRACAS: A capacity spectrum approach for seismic fragility assessment including record-to-record variability" *Engineering Structures*, 125, 337–348.

Scott, M.H., Fenves, and G.L. (2006). "Plastic hinge integration methods for force-based beam-column elements" *Journal of Structural Eng.*, 132(2), 244–252.

Scozzese, F., Dall'Asta, A., and Tubaldi, E. (2019). "Seismic risk sensitivity of structures equipped with anti-seismic devices with uncertain properties" *Structural Safety*, 77, 30–47.

Smerzini, C., Galasso, C., Iervolino, I., and Paolucci, R. (2014). "Ground motion record selection based on broadband spectral compatibility" *Earthquake Spectra*, 30 (4), 1427–1448.

Tubaldi E, Barbato M, and Dall'Asta A (2016). "Efficient approach for the reliability-based design of linear damping devices for seismic protection of buildings" *ASCE-ASME Journal of Risk and Uncertainty in Engineering Systems: Part A-Civil Eng.*, *2*(2), C4015009.

Uang CM, and Nakashima M (2004). "Steel buckling-restrained braced frames" *In Earthquake Engineering: from Engineering Seismology to Performance-based Engineerin*g, Bozorgnia Y, Bertero VV (eds.), CRC Press: Boca Raton, FL.

Zona, A., Ragni, L., and Dall'Asta A. (2012). "Sensitivity-based study of the influence of brace over-strength distributions on the seismic response of steel frames with BRBs." *Engineering Structures*, 37(1), 179–192.

Zona, A., and Dall'Asta, A. (2012). "Elastoplastic model for steel buckling-restrained braces." *Journal of Constructional Steel Research*, 68(1), 118–125.